Design of an Organic Ultramicroelectrode Array. Potential Use of Microstructures of Binary Langmuir–Blodgett Monolayers of Totally π-Conjugated Electroactive and Electroinactive Amphiphiles

Masashi Kunitake,# Kenji Nasu, Yoshitaka Narikiyo, Osamu Manabe, and Naotoshi Nakashima*

Department of Applied Chemistry, Faculty of Engineering, Nagasaki University, Bunkyo-cho, Nagasaki 852

(Received March 8, 1995)

Mixed monolayers of totally π-conjugated electroactive compounds, 1-methyl-4-[2-[4-[2-(4-quinolyl)vinyl]phenyl]vinyl]quinolinium perchlorate (**1**) and 1-methyl-4-[2-[4-[2-(4-pyridyl)vinyl]phenyl]vinyl]pyridinium perchlorate (**2**) and those of compound **1** and palmitic acid (**PA**) were formed on a 0.1 M $KClO_4$ aqueous solution. Surface pressure area isotherms and fluorescence microscopic observations suggest that mixtures of compounds **1** and **2** form homogeneous mixed monolayers, but those of **1** and **PA** are phase-separated in the mixed monolayers. These monolayers were transferred to gold by using the Langmuir–Blodgett technique and then in situ electrochemical characterization was conducted. Cyclic voltammograms of the mixed monolayers of **1-2** and **1-PA** on gold indicate rectified transmembrane electron transfer through the monolayer of **1** in the mixed monolayers to hexacyanoferrate(II) in solution. Potential-step chronocoulometric responses have revealed that the monolayer of **1** in the mixed LB monolayer of **1-2** acts as an organic ultramicroelectrode array electrode.

The formation and characterization of assembled organic monolayers, especially those possessing electroactive moieties, on electrodes are of considerable interest because they provide organized and oriented electrochemical reaction sites on metal electrode surfaces.[1—20] A convenient way to form monolayers on electrode surfaces is the use of self-assemblies of alkanethiols and their derivatives with a long alkyl chain from solution onto gold surfaces.[21,22] Using this approach, the surface coverage of monolayers on gold can be roughly controlled by changing the immersion time of the gold electrodes in the thiol-containing organic solution and the concentration of thiol in the organic solvent. These monolayers can be prepared with relatively defect-free structures. In self-assembly procedures, the control of the composition ratio in mixed monolayers is not easy. Langmuir–Blodgett (LB) film transfer is an alternative technique for the formation of monolayers on solid substrates.[23] Although LB monolayers on solid surfaces often retain defect structures from the monolayers formed at the air-water interface, the LB technique is a powerful method for the formation of multicomponent monolayers *with different composition ratios* on solid surfaces.

The purpose of this study is the design and preparation of an organic ultramicroelectrode array using microstructures of LB monolayers for the stepwise electron transfer through totally π-conjugated electroactive compounds. There are some reports of the formation of monolayer-based ultramicroelectrodes for the study of very rapid electrode kinetics. Sabatini and Rubinstein[24] studied the microelectrode kinetics of an ultramicroelectrode array of self-assembled monolayers formed spontaneously by adsorption of octadecyltrichlorosilane and 1-octadecanol on gold. Bilewicz and Majda[25] reported the formation of mixed LB films of octadecylmercaptan and octadecylalcohol containing ubiquinone which act as a "gate site" for the electrochemical communication with $[Ru(NH_3)_6]^{3+/2+}$ in solution. Detailed electrochemical studies of self-assembled octadecylmercaptan monolayers on gold as microarray electrodes were described by Finklea, Rubinstein and co-workers.[26]

Very recently, we described the formation of monolayers of π-conjugated electroactive compounds (**1**, **2**) at the air–water interface and rectified transmembrane electron transfer through the LB monolayers of **1** and **2** on gold with $[Fe(CN)_6]^{3-}$ in solution (Chart 1).[17] The study led us to design and develop organic ultramicroar-

#Present address: Itaya Electrochemiscopy Project, JRDC, Yagiyama-minami, Taihaku-ku, Sendai 980.

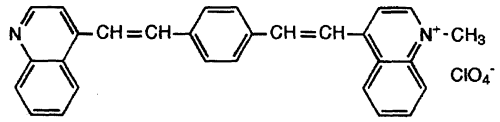

1

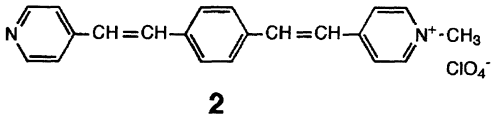

2

$CH_3(CH_2)_{14}COOH$

PA

Chart 1.

rays using LB monolayers of π-conjugated electroactive amphiphiles on electrodes, as described here.

Experimental

Materials. The syntheses of 1-methyl-4-[2-[4-[2-(4-quinolyl)vinyl]phenyl]vinyl]quinolinium perchlorate (**1**) and 1-methyl-4-[2-[4-[2-(4-pyridyl)vinyl]phenyl]vinyl]pyridinium perchlorate (**2**) were described elsewhere.[17] Palmitic acid (**PA**) was recrystallized twice from ethanol solution before use.

Surface Pressure-Area Isotherms. Surface pressure-area isotherms of the single component and mixed monolayers of **1**, **2**, and **PA** were measured on a 0.1 M (1 M=1 mol dm^{-3}) $KClO_4$ Milli-Q aqueous solution (20 °C) at a compression rate of 40 mm min^{-1} by a computer-controlled film balance (USI System, Model FSD-110). Acetonitrile/benzene (v/v=1/9, Tokyo Kasei spectroscopic grade) was used as the spreading solvent.

Fluorescence Microscopic Observation of Monolayers. The fluorescence microscopy setup used in this study includes a computer-controlled film balance (USI System, FSD-110) and a fluorescence microscope equipped with a SIT TV camera (Hamamatsu Photonics, Model C-2400) and a video recording system.[27] A 150 W Hg lamp with a filter (Zeiss, BP546/12) was used for excitation, and the light emitted from a monolayer was passed through a filter (Zeiss, LP590). Compound **1** was found to be fluorescent, therefore, addition of a fluorescence probe such as octadecylrhodamine B to the monolayers was not necessary in this study.

Formation of LB Monolayer Electrodes. A computer-controlled Langmuir–Blodgett trough (size: 330×40 mm^2, maximum barrier moving area: 300×40 mm^2) equipped with an area controller (USI System Co., Ltd., FSD-111) was used for the preparation of the monolayer electrodes. The trough was placed in a closed box containing nitrogen. The deposition of the monolayers was conducted with the modified horizontal dipping procedure, typically as follows. At a surface pressure of 20 mN m^{-1}, a well-polished Au disk electrode (Bioanalytical Systems, diameter 1.6 mm) was slowly lowered to make contact with the monolayer at the air/water interface for about 10 s. The electrode was then further lowered into the subphase (obtained monolayer electrodes: **1**/Au, **2**/Au, **1-2**/Au, **1-PA**/Au).

In Situ Electrochemical Measurements of LB Monolayer Modified Electrodes. In situ cyclic voltammetry and potential-step chronocoulometry of the modified electrodes were conducted in the subphase solution with an electrochemical analyzer (Bioanalytical Systems, 100B) in a closed box under a nitrogen atmosphere. A saturated calomel electrode and a Pt wire were used as the reference and the counter electrodes, respectively. The experimental conditions of potential-step chronocoulometry were as follows. The solutions were all deoxygenated 0.1 M $KClO_4$ containing 0.01 M $K_3[Fe(CN)_6]$. The initial and final potentials were 0.5 V and −0.75 V, respectively and the pulse width was 200 ms. For the diffusion constant of $[Fe(CN)_6]^{3-}$, the reported value of 7.69×10^{-6} cm^2 s^{-1} was used.

Results and Discussion

As we have described elsewhere,[17] the totally π-conjugated compounds **1** and **2** showed typical expanded monolayers at the air/water interface. Figure 1 shows the surface pressure-area isotherms of the mixed monolayers composed of **1-2** and **1-PA** at 20 °C. The limiting areas occupied by **1** and **2** on 0.1 M $KClO_4$ aqueous solution at 20 °C were 0.37 and 0.27 nm^2/molecule, respectively. These values are almost identical with areas estimated from CPK space-filling models. Figure 2 shows plots of the area of mixed monolayers composed of **1-2** and **1-PA** at a surface pressure of 25 mN m^{-1} as a function of mole fraction of compound **1**.[27–29] When compound **1** was mixed with compound **2**, there was

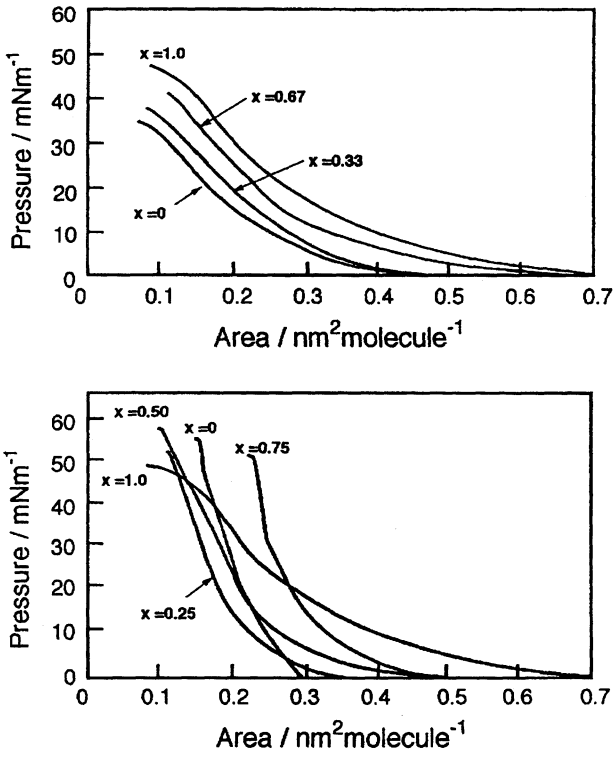

Fig. 1. Surface pressure-area isotherms for binary monolayers of **1-2** (above) and **1-PA** (below) on 0.1 M $KClO_4$ aqueous solutions at 20 °C. X is the mole fraction of **1** in the LB monolayers.

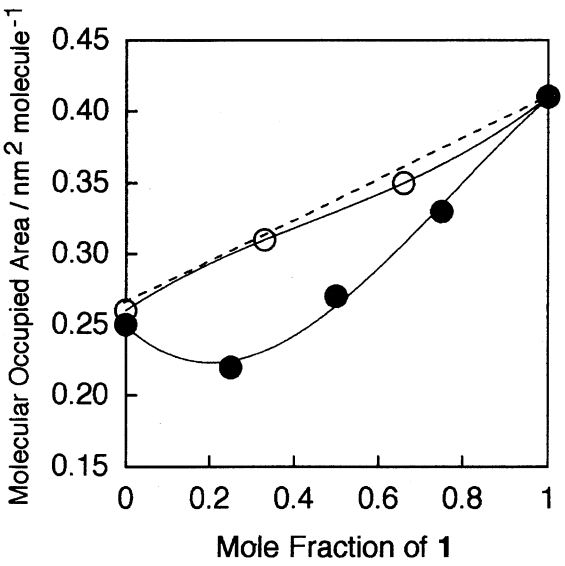

Fig. 2. Plots of mean molecular occupied area for **1-2** (○) and **1-PA** (●) monolayers calculated from the data (at 25 mN m^{-1}) of Fig. 1 as a function of mole fractions of **1**. See the text for details.

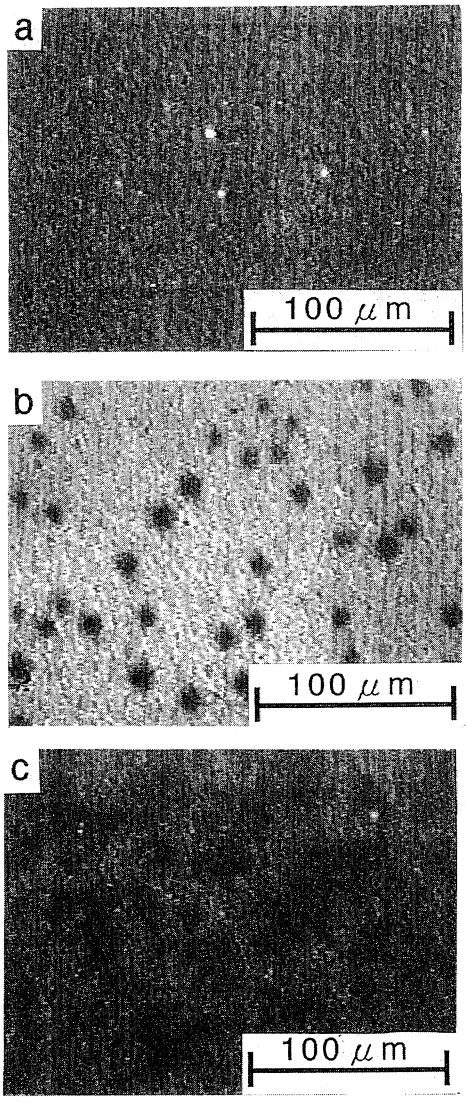

Fig. 3. Fluorescence microscopic images of mixed monolayers of **1-2** and **1-PA** on a 0.1 M $KClO_4$ aqueous solution at 20 °C. a. **1-2** monolayer (molar ratio; **1/2**=1, surface pressure; 20 mN m^{-1}), b. **1-PA** monolayer (molar ratio; **1/PA**=1, surface pressure; 0 mN m^{-1}), c. **1-PA** monolayer (molar ratio; **1/PA**=1, surface pressure; 20 mN m^{-1}).

no deviation from the expected theoretical straight line (dotted) which occurs in the case of ideal mixing or complete non mixing. Because the chemical structures of **1** and **2** are similar, "semi-quantitative ideal" mixing is suggested. In contrast, when compound **1** was mixed with **PA**, a considerable negative deviation from ideal mixing, associated with a strong molecular interaction between each component molecule, was observed.

In order to obtain direct images of the structures of the binary monolayers at the air/water interface, we applied a fluorescence microscopic technique.[27,30,31] Fluorescence micrographs of the monolayers of **1-2** and **1-PA** at 20 °C are shown in Fig. 3. In the applied excited condition, only compound **1** fluorescence was observed. At surface pressures of zero (data not shown) and 20 mN m^{-1}, totally homogeneous microscopic images were observed for the **1-2** monolayers (Fig. 3a), indicating that the two components were uniformly mixed. In contrast, the **1-PA** mixed monolayer gave darks spot at 0 mN m^{-1} (Fig. 3b) and an increase in the surface pressure to 20 mN m^{-1} led to enlarged domains in the matrix (Fig. 3c). Despite the strong molecular interaction between compounds **1** and **PA**, as can be seen from Fig. 2, phase separation behavior between the two component is evident. This can be explained as follows: the two components interact at the molecular level, but at the macroscopic level (μm size), phase separation occurs between the single component of compound **1** and the mixed phase of **1** and **PA** or the single phase of **PA** and the mixed phase of **1** and **PA**. The former explanation is suggested from the electrochemical results described below.

Each mixed monolayer of **1-2** and **1-PA** was transferred to a gold disk electrode by lowering a polished electrode horizontally to the air/water interface at 20 mN m^{-1} and then pushing it into the subphase (0.1 M $KClO_4$) to conduct in situ electrochemistry.

Single-component monolayers of **1** and **2** on gold electrodes give cyclic voltammograms with $E_{pa}=-0.78$ V, $E_{pc}=-0.84$ V and $E_{pa}=-0.86$ V, $E_{pc}=-1.08$ V, respectively.[17] These redox couples are attributable to the one-electron reduction/oxidation couple of **1** and **2**. Typical *i*–*E* curves (first scan) of a mixed monolayer modified electrode of **1-2** (**1/2**=0.5) are shown in Fig. 4. The switching potential was set to −0.90 V in order to measure the redox current of compound **1** only in the mixed monolayer on the electrode; i.e., the electrochemistry of amphiphile **2** is almost negligible. Transmembrane vectorial electron transfer to a redox

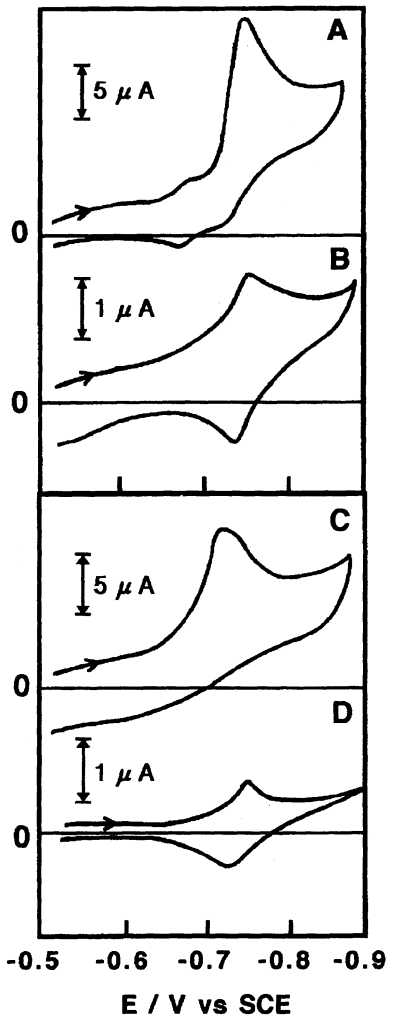

Fig. 4. Cyclic voltammograms for binary monolayer electrodes modified with **1-2** (A and B) and **1-PA** (C and D) in the presence (A and C) and the absence (B and D) of 1 mM $K_3[Fe(CN)_6]$ in deoxygenated 0.1 M $KClO_4$ solution. Measured potential range: −0.5 to −0.9 V vs. SCE. Scan rate, 0.2 $V s^{-1}$. Molar ratios of **1/2** and **1/PA** are both 0.5.

species in solution via π-conjugated compound **1** in the mixed monolayers was examined. In the presence of ferricyanide, a **1-2**/Au electrode gave minimal faradaic electrochemistry near 0.2 V vs. SCE, the formal potential of ferricyanide (Fig. 5, trace b). This indicates that the mixed monolayer blocks the direct electrochemical communication of ferricyanide with the electrode. It is evident by comparing trace a and trace b in Fig. 4 that the presence of ferricyanide results in an increase in the cathodic current and the disappearance of the anodic current near −0.75 V. This demonstrates a one-way electron transfer from **1** in the mixed monolayer to $[Fe(CN)_6]^{3-}$ in solution. Moreover, the stepwise electron transfer via **1** molecules in the mixed monolayer assemblies on the electrode to $[Fe(CN)_6]^{3-}$ in the subphase is indicated. A **1-PA**/Au mixed monolayer electrode gave similar *i-E* curves (Fig. 4, c and d); however, the

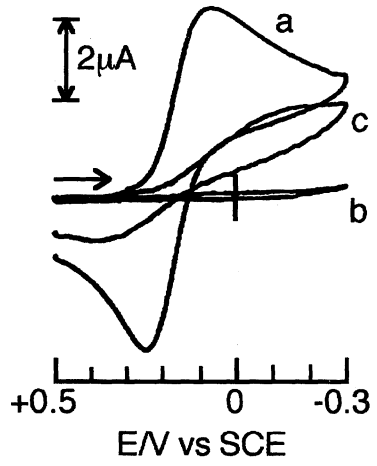

Fig. 5. Cyclic voltammograms for a bare electrode (a) and the same monolayer modified electrodes as in Fig. 4 (b, **1-2**; c, **1-PA**) in the presence of 1 mM $K_3[Fe(CN)_6]$ in deoxygenated 0.1 M $KClO_4$ solution. Measured potential range: +0.5 to −0.3 V vs. SCE. Scan rate, 0.2 $V s^{-1}$.

blocking ability of the monolayer on the electrode for the direct electron transfer between the electrode and $[Fe(CN)_6]^{3-}$ was poor (Fig. 5, trace c). In the **1-PA** system, blocking ability was increased with the increase of the composition ratios of **PA**.

Potential-step chronocoulometry[32] was used to examine the phase structure of the binary monolayer modified electrodes with different molar ratios of **1/2** and **1/PA**. Figure 6 shows typical chronocoulometric responses for the **1-2**/Au electrode in the form of Anson plots. The value of "A", defined as the apparent "effective" electrode area for the mixed monolayer with different molar ratios on modified electrodes, and the value of "A^0 ", defined as the apparent electrode area of the pure **1** monolayer modified electrode, can be calculated from those Anson plots for the **1-2**/Au and **1-PA**/Au electrodes using the following equation:

$$Q = 2nFAD_0^{1/2}C_0^* t^{1/2}, \quad (1)$$

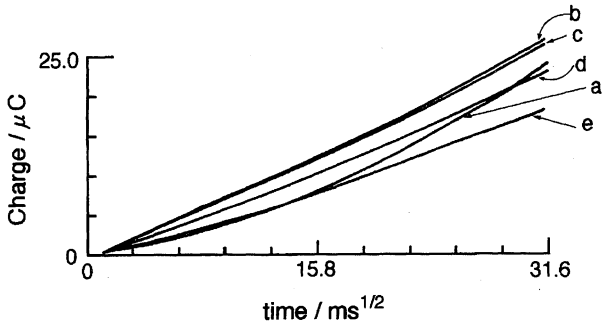

Fig. 6. Chronocoulometric Anson plots for mixed monolayers of **1-2** on gold in the presence of 0.01 M $K_3[Fe(CN)_6]$ in deoxygenated 0.1 M $KClO_4$ aqueous solution at 20°C. Mole fractions of **1** are: 1.0 (a), 0.5 (b), 0.4 (c), 0.2 (d), 0.1 (e).

where Q, n, F, D_0, and C_0^* are the charge, the electrons per molecules oxidized or reduced, the Faraday number, the diffusion coefficient, and the bulk concentration of the electroactive species, respectively.[33] Table 1 summarizes the slopes, $Qt^{1/2}$, of the Anson plots and the apparent electrode areas for **1**/2/Au and **1**+**PA**/Au electrodes with different fractions of **1**. In Fig. 7, A/A^0 ratios for the mixed monolayer modified electrodes are plotted as a function of the mole fraction of **1**. In the mixed monolayer system of **1-2**, A/A^0 changed very little; i.e., the value of A/A^0 for the monolayer of **1-2** at a mole fraction 0.4 showed just a 10% decrease compared with a mole fraction of 1.0. On the other hand, in the mixed monolayers of **1-PA**, A/A^0 values decreased almost linearly with a decrease in the composition ratio of **1**. But the extrapolation of the plot of A/A^0 vs. the mole fraction of **1** does not give a zero intercept. This may be due to insufficient blocking of these monolayers toward ferricyanide.

The differences in the electrochemistry between the two kinds of mixed monolayer systems can be explained by differences in diffusion mechanisms. At the **1-PA** mixed monolayer modified electrodes, the distances between the formed electroactive domains of **1** on Au may be large in comparison with the thickness of the diffusion layer.[34] Thus, the electrochemistry is being controlled by linear diffusion, which gives a linear relationship between A/A^0 and the mole fraction of **1**. At the **1-2** mixed monolayer electrodes, distances between the electroactive domains of **1** in the mixed monolayer are expected to be smaller than those of the diffusion layer. This is because **1-2** forms "semi-quantitative ideal" mixed monolayers and radiation diffusion is operative;[35—37] i.e., the apparent diffusion layer does not decrease linearly with the decrease in the mole fraction of **1**. The results of Fig. 7 for a **1-2** monolayer electrode are consistent with this model. Radial diffusion depends on whether the diffusion layers overlap and the layer thickness depends on time.

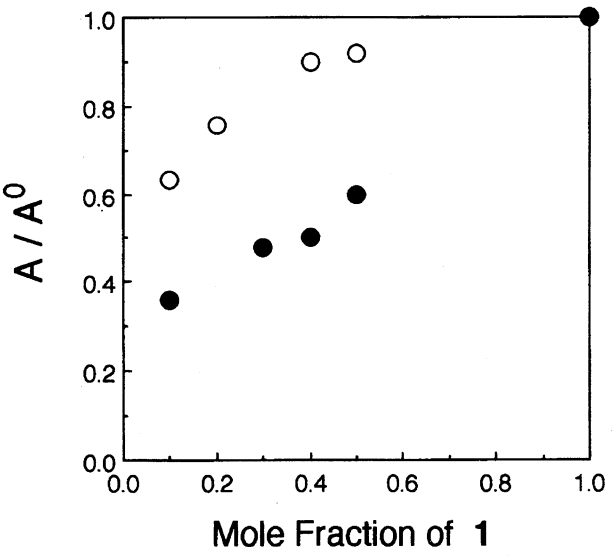

Fig. 7. Electrode area rations (A/A^0) for the mixed monolayer modified electrodes obtained from Anson plots (Fig. 6) as a function of the mole fraction of **1**. Open circles: **1-2** modified electrodes, solid circles: **1-PA** electrodes.

Conclusions

A new type of organic ultramicroelectrode array using mixed Langmuir–Blodgett monolayers of electroactive and electroinactive π-conjugated amphiphiles has been described. Stepwise rectified transmembrane electron transfer which exhibits microelectrode behavior occurs through electroactive molecules in mixed monolayer assemblies on electrodes to $[Fe(CN)_6]^{3-}$ in bulk solution. Cyclic voltammetry and potential-step chronocoulometry have been used to characterize these reactions. Microstructures of the ultramicroelectrode arrays could be controlled by the miscibility of the binary components in the monolayer assemblies on the water surfaces.

To the best of our knowledge, this is the first report on the preparation and electrochemical characterization of an organic ultramicroelectrode array using binary LB monolayers of π-conjugated electroactive and electroinactive compounds. Totally π-conjugated compounds are candidates for "molecular wires"[38,39] which connect electron flow between the different elements of a molecular electronic device. The present study may be useful in such applied fields apart from the fundamental aspects of this work.

Table 1. $Q/t^{1/2}$ and Apparent Electrode Area for **1**+**2**/Au and **1**+**PA**/Au Electrodes

Fraction of **1**	1/1+2		1/1+PA	
	$Q/t^{1/2}$ coulomb/s$^{1/2}$	Apparent electrode area, A/mm^{2}[a]	$Q/t^{1/2}$ coulomb/s$^{1/2}$	Apparent electrode area, A/mm^{2}[b]
1.0	0.977	1.02(=A^0)	0.293	1.03(=A^0)
0.5	0.872	0.913	0.178	0.621
0.4	0.853	0.893	0.148	0.516
0.3	[c]	—	0.142	0.495
0.2	0.717	0.750	[c]	—
0.1	0.620	0.648	0.106	0.366

a) $[Fe(CN)_6]^{3-}$=10 mM. b) $[Fe(CN)_6]^{3-}$=3 mM. c) Not measured.

We are very grateful to Professor T. Kunitake and Professor S. Shinkai for the use of the film balances equipped with the fluorescence microscope. This work was supported, in part, by the Isumi Science and Technology Foundation, the General Sekiyu Research & Development Encouragement & Assistance Foundation and a Grant-in-Aid for Science Research from the Ministry of Education, Science and Culture.

References

1) H. Daifuku, K. Aoki, K. Tokuda, and H. Matsuda, *J. Electroanal. Chem.*, **183**, 1 (1985).
2) H. Daifuku, I. Yoshimura, I. Hirata, K. Aoki, K. Tokuda, and H. Matsuda, *J. Electroanal. Chem.*, **199**, 47 (1986).
3) M. Fujihira and T. Araki, *Bull. Chem. Soc. Jpn.*, **59**, 2375 (1986).
4) a) C.-W. Lee and A. J. Bard, *J. Electroanal. Chem.*, **239**, 441 (1988); b) C. J. Miller and A. J. Bard, *Anal. Chem.*, **63**, 1707 (1991); c) Y. S. Obeng, M. E. Laing, A. C. Friedli, H. C. Yang, D. Wang, E. W. Thulstrup, A. J. Bard, and J. Michl, *J. Am. Chem. Soc.*, **114**, 9943 (1992).
5) a) S. E. Creager, D. M. Collard, and M. A. Fox, *Langmuir*, **6**, 1617 (1990); b) S. E. Creager and G. K. Rowe, *J. Electroanal. Chem.*, **370**, 203 (1994).
6) M. Kunitake, K. Akiyoshi, K. Kawatana, N. Nakashima, and O. Manabe, *J. Electroanal. Chem.*, **292**, 277 (1990).
7) C. E. D. Chidsey, C. R. Bertozzi, T. M. Putvinski, and A. M. Mujsce, *J. Am. Chem. Soc.*, **112**, 4301 (1990).
8) D. H. Charych, M. E. Landau, and M. Majda, *J. Am. Chem. Soc.*, **113**, 3340 (1991).
9) S. Ueyama and S. Isoda, *J. Electroanal. Chem.*, **310**, 281 (1991).
10) M. Kunitake, S. Kawahara, N. Nakashima, and O. Manabe, *J. Electroanal. Chem.*, **309**, 241 (1991).
11) J. Li and E. A. Kaifer, *Langmuir*, **9**, 591 (1993).
12) H. O. Finklea and D. D. Hanshew, *J. Electroanal. Chem.*, **347**, 327 (1993).
13) E. Katz, N. Itzhak, and I. Wilner, *Langmuir*, **9**, 1392 (1993).
14) a) Y. Sato, H. Itoigawa, and K. Uosaki, *Bull. Chem. Soc. Jpn.*, **66**, 1032 (1993); b) K. Shimazu, I. Yagi, Y. Sato, and K. Uosaki, *J. Electroanal. Chem.*, **372**, 117 (1994).
15) a) W. B. Caldwell, K. Chen, C. A. Mirkin, and S. J. Rabinec, *Langmuir*, **9**, 1945 (1993); b) K. Chen, W. B. Caldwell, and C. A. Mirkin, *J. Am. Chem. Soc.*, **115**, 1193 (1993).
16) X. Tang, T. Schneider, and D. A. Buttry, *Langmuir*, **10**, 2235 (1994).
17) M. Kunitake, K. Nasu, O. Manabe, and N. Nakashima, *Bull. Chem. Soc. Jpn.*, **67**, 375 (1994).
18) S. Creager and G. A. Rowe, *J. Electroanal. Chem.*, **370**, 203 (1994).
19) D. Aceredo, R. L. Bretz, J. D. Tirado, and H. D. Abruna, *Langmuir*, **10**, 1300 (1994).
20) B. R. Herr and C. A. Mirkin, *J. Am. Chem. Soc.*, **116**, 1157 (1994).
21) R. G. Nuzzo and D. L. Allara, *J. Am. Chem. Soc.*, **105**, 4481 (1983).
22) a) A. Ulman, "An Introduction to Ultrathin Organic Films from Langmuir–Blodgett to Self-Assembly," Academic Press, San Diego (1991); b) J. F. Facci, "In Modern Design of Electrode Surfaces," ed by R. W. Murray, Wiley-Interscience Publication, New York (1992), pp. 119—158.
23) G. Roberts, "Langmuir-Blodgett Films," Plenum Press, New York (1990).
24) E. Sabatani and I. Rubinstein, *J. Phys. Chem.*, **91**, 6663 (1987).
25) a) R. Bilewicz and M. Majda, *J. Am. Chem. Soc.*, **113**, 5464 (1991); b) *Langmuir*, **7**, 2794 (1991).
26) H. O. Finklea, D. A. Snider, J. Fedyk, E. Sabatani, Y. Gafni, and I. Rubinstein, *Langmuir*, **9**, 3360 (1993).
27) L. F. Chi, R. R. Johnston, H. Ringsdorf, N. Kimizuka, and T. Kunitake, *Langmuir*, **8**, 1360 (1992).
28) B. A. Cornell, M. M. Sacrè, W. E. Peel, and D. Chapman, *FEBS Lett.*, **90**, 29 (1978).
29) F. C. Goodrich, "Proc. 2nd Int. Congr. Surface Activity," London (1957), p. 85.
30) H. M. McConnell, K. Tamm, and R. M. Weis, *Proc. Natl. Acad. Soc. U.S.A.*, **81**, 3249 (1984).
31) M. Lösche, E. Sackmann, and H. Möhwald, *Ber. Bunsenges. Phys. Chem.*, **87**, 848 (1984).
32) A. J. Bard, Faulkner, "Electrochemical Method," Wiley, New York (1980), Chap. 5.
33) Chronocoulometric responses at 300—1000 ms were used in the calculation of diffusion coefficients.
34) Estinated thickness of the diffusion layer is 49 μm.
35) H. Reller, E. K.-Eisner, and E. Gileadi, *J. Electroanal. Chem.*, **138**, 65 (1982).
36) C. Amatore, J. M. Savéant, and D. Tesseier, *J. Electroanal. Chem.*, **147**, 39 (1983).
37) "Ultramicroelectrodes," ed by M. Fleischman, S. Pons, D. R. Rolison, and P. Schmidt, Datatech Systems, Inc., Science Publishers, 1987.
38) a) T. S. Arrhenius, M. B.-Desce, M. Dvolaitzky, and J.-M. Lehn, *Proc. Natl. Acad. Sci. U.S.A.*, **83**, 5355 (1986); b) S. Kugimiya, T. Lazrak, M. B.-Desce, and J.-M. Lehn, *J. Chem. Soc., Chem. Commun.*, **1991**, 1179; c) J.-M. Lehn, *Angew. Chem., Int. Ed. Engl.*, **29**, 1304 (1990).
39) F. Effenberger, P. Meller, H. Ringsdorf, and H. Schlosser, *Adv. Mater.*, **3**, 555 (1991).